applied sciences

MDPI

Article

Convergence Analysis of the Phase-Scheduled-Command FXLMS Algorithm with Phase Error

Yushuai Wang [1,*], Feng Liu [2], Zhenrong Fu [1], Lianxin Yang [1] and Pengfei Wang [1]

[1] College of Mechatronic Engineering, North University of China, Taiyuan 030051, China; fuzhenrong2022@163.com (Z.F.); yanglianxin0314@163.com (L.Y.); wangpf20210001@nuc.edu.cn (P.W.)
[2] China Orient Institute of Noise and Vibration, Beijing 100085, China; liuf@coinv.com
* Correspondence: wangys@nuc.edu.cn

Abstract: In this paper, a phase-scheduled-command filtered-x least mean square (FXLMS) algorithm with a phase error between the disturbance and command signal is analyzed in detail. The influence of the phase error on the control effort, convergence time constant and performance of convergence is explained for both stationary and nonstationary disturbance signal cases. An estimation ratio, in both stationary and nonstationary disturbance cases, of the pseudo-error MSE convergence performance is also developed and discussed. Simulation results were collected to verify the analysis. The results show that, for both stationary and nonstationary disturbance, the phase error may heavily increase the distance of the optimum vector from the initial value, leading to a large control effort, a large convergence time constant and poor convergence performance. The estimation ratio also has a satisfactory performance for estimating the influence of the phase error.

Keywords: active noise control; phase-scheduled-command FXLMS; active sound profiling; phase error

check for updates

Citation: Wang, Y.; Liu, F.; Fu, Z.; Yang, L.; Wang, P. Convergence Analysis of the Phase-Scheduled-Command FXLMS Algorithm with Phase Error. *Appl. Sci.* **2023**, *13*, 8797. https://doi.org/10.3390/app13158797

Academic Editor: Lamberto Tronchin

Received: 5 June 2023
Revised: 23 July 2023
Accepted: 28 July 2023
Published: 30 July 2023

Copyright: © 2023 by the authors. Licensee MDPI, Basel, Switzerland. This article is an open access article distributed under the terms and conditions of the Creative Commons Attribution (CC BY) license (https://creativecommons.org/licenses/by/4.0/).

1. Introduction

In specific acoustic environments, such as the interior of a car, the customer-perceived quality of sound has gradually come to be considered important. It is well known that noise control involves some sounds being tuned to enhance the vehicle sound quality, invoking some desired emotional response, while others should be suppressed to reduce annoyance [1]. Therefore, in such a case, the goal of noise control is, not only to eliminate noise, but to control the noise at a specific level, which is known as sound quality control. With the benefit of the action of a secondary noise source in an active noise control (ANC) system, the amplitude of sound can be tuned to a specific level. Therefore, active sound quality control systems based on ANC algorithms provide the possibility of dealing with the problem by equalizing or profiling the sound [2–7].

There are two schemes for the active sound quality control system based on the FXLMS algorithm: active noise equalizer (ANE) [8–12] and active sound profiling (ASP) algorithms [13–16]. The ANE, first presented by Kuo et al. [8,9], can either enhance or eliminate the sound level by the insertion of gain factors and the balancing branch, ensuring that the actual noise converges to a desirable value, tuned by gain factor β. Based on the ANE technique, Kuo et al. [17–19] proposed an optimized filtered-error least mean square (FELMS) scheme, which improved the convergence speed and system stability, and a frequency domain delayless active sound quality control (ASQC) structure which was more efficient, faster and had lower computational complexity compared to time-domain algorithms. In view of this, Oliveira et al. [20] developed an NEX-LMS-scheme ASQC algorithm by changing the gain factor with the frequency components for the application of equalization of engine noise. The performance of the NEX-LMS scheme was experimentally validated, and it worked effectively when the frequency was slowly increased. Additionally, Mosquera-Sanchez et al. [21–23] introduced a frequency domain multichannel ANE scheme for independent sound control of multiple locations, and a system to control the loudness,

roughness, sharpness and tonality of noise. The performance of the control schemes was verified through simulations and experiments. The ANE-based algorithms have been employed as a popular and important sound-equalizing method. Their performance has been studied, and it has been concluded that they are extremely sensitive to misestimation of the secondary path. The phase misestimation influence is dominant when β is small, and the amplitude misestimation influence becomes dominant when $\beta > 1$ [13,24]. To fundamentally prevent the influence of the secondary model misestimation, Rees et al. [13] proposed an alternative active sound profiling (ASP) scheme, which was characterized by converging the residual signal to a generated command value signal. The command value signal was set with the desirable value amplitude and the same frequency as the reference signal. A pseudo-error signal was used to update the adaptive filter weights, and the real residual noise signal converged to the command signal as the pseudo-error converged to zero. Further, to limit the control effort, the command signal was set to be in phase with the primary disturbance signal, and the phase-scheduled-command FXLMS (PSC-FXLMS) sound profiling algorithm can be derived. The command signal is created at the frequency corresponding to the reference signal, which ensures that its frequency components are the same as the disturbance signal. The command signal phase is set by the measured phase by performing a fast Fourier transform (FFT) on the modeled disturbance. However, the modeled disturbance may be influenced by broadband signals, such as road noise, resulting in an error of the measured phase. Based on the PSC-FXLMS algorithm, several modifications and improvements have been proposed to address the plant model stability under errors, the convergence speed and the influence of control effort for phase error between the disturbance and command signals [13,14]. To address a limitation of these ASP algorithms, that they are always effective for stationary noise conditions, Wang et al. [15] proposed an algorithm for nonstationary noise profiling application. This algorithm inherits the advantages of minimum control effort and insensitivity to the magnitude error of a plant model.

A detailed investigation is important and useful to understand the behavior of ANE-based and ASP-based algorithms, and stimulate and inspire the development of more advanced and practical ANC system structures and algorithms for sound quality control. Detailed investigations of ANE-based algorithms have been widely reported in references [13,16,24,25]. They have drawn the following conclusions: when the gain factor is small, the influence of the secondary path phase estimation error is dominant; however, when the gain factor is larger than one, the influence of the secondary path amplitude estimation error becomes dominant.

For the ASP-based algorithm, Rees et al. [13] provided a qualitative guide of properties, including the plant model stability and the influence of control effort with phase error between the disturbance and command signals. However, the convergence time constant and convergence performance of the influence of phase error between disturbance and command signal has not been particularly considered. Therefore, in this paper, for both stationary and nonstationary disturbance cases, a detailed analysis of the classical ASP-based algorithm (PSC-FXLMS) considering the convergence time constant and convergence performance with phase error between disturbance and command signal is conducted.

The rest of this paper is organized as follows. Section 2 provides a brief introduction to the PSC-FXLMS algorithms. Section 3 conducts the performance analysis of this system with phase error between the disturbance and command signal. Section 4 presents some simulations to demonstrate the validity of the analytical findings. Conclusions are provided in Section 5.

2. Active Sound Profiling Algorithms

2.1. Command-FXLMS Algorithm

A schematic of the command-FXLMS algorithm is presented in Figure 1, where it can be seen that the command signal $c(n)$ is the predefined value target for the residual error signal $e(n)$. The command signal is created from the reference signal, which ensures that

the frequency components of the command signal are the same as those of the disturbance signal. The pseudo-error $e'(n)$, instead of the residual error signal $e(n)$, is introduced for updating the adaptive filter. As the pseudo-error $e'(n)$ converges to zero with the updating of the algorithm, the residual error signal $e(n)$ converges to the command signal $c(n)$ which indicates the predefined value.

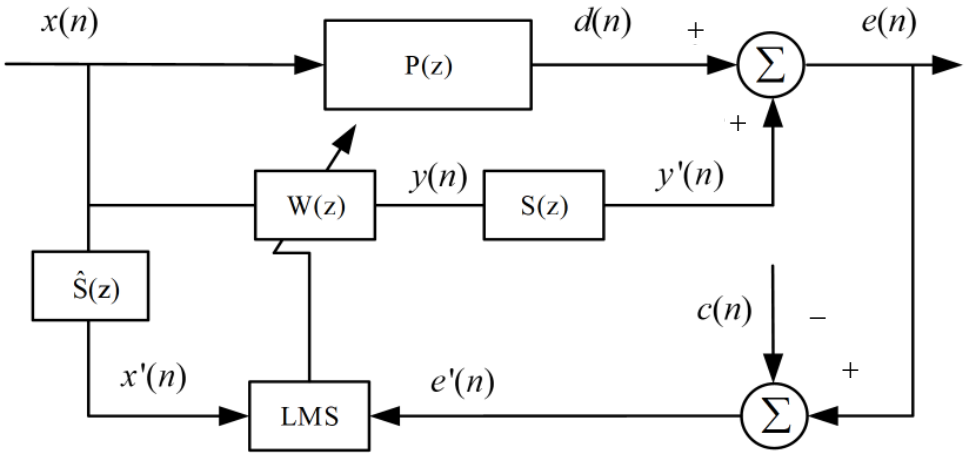


Figure 1. Block diagram of the command-FXLMS algorithm.

As is shown in Figure 1, the error noise $e(n)$ can be calculated by

$$e(n) = d(n) + y'(n) = d(n) + s(n) * y(n) \tag{1}$$

where $d(n)$ is the disturbance signal, $y'(n)$ is the counter noise signal, $s(n)$ is the impulse response of the FIR filter $S(z)$ of the secondary path and $y(n)$ is the output of the adaptive filter $W(z)$, for which it is given by

$$y(n) = \mathbf{w}^T(n)\boldsymbol{x}(n) \tag{2}$$

where the $x(n)$ is the reference signal vector and the superscript "T" denotes the transpose of a matrix. The vector $\mathbf{w}(n)$ is the adaptive weight vector of the least mean square (LMS) algorithm, and its iteration follows the method of steepest descent and can be expressed as

$$\mathbf{w}(n+1) = \mathbf{w}(n) + \mu \boldsymbol{x}'(n)e'(n) \tag{3}$$

where μ is the step size, $\mathbf{x}'(n)$ is the filtered reference signal and can be expressed by

$$\mathbf{x}'(n) = [x'(n) \quad x'(n-1) \quad \cdots \quad x'(n-L+1)] \tag{4}$$

where L is the length of vector, and the value of $x'(n-l)$ is obtained by

$$x'(n-l) = x(n-l) * \hat{s}(n) \tag{5}$$

where $l = 0, 1, \ldots L-1$, $\hat{s}(n)$ is the impulse response of the modeled FIR filter $\hat{S}(z)$ of the secondary path. The $e'(n)$ is the pseudo-error signal, which is expressed by

$$e'(n) = e(n) - c(n) \tag{6}$$

It can be seen that when the pseudo-error signal converges to zero, the residual error signal $e(n)$ converges to the command signal $c(n)$ which indicates the predefined value.

2.2. PSC-FXLMS Algorithm

In practical applications, the command-FXLMS algorithm is highly robust to amplitude errors in the plant estimates, which represents a significant advantage over the ANE-based

algorithms. However, this algorithm has excessive control effort if the command and disturbance signals are out of phase. To overcome this shortcoming, Rees et al. [13] have proposed the PSC-FXLMS algorithm, which is shown in Figure 2.

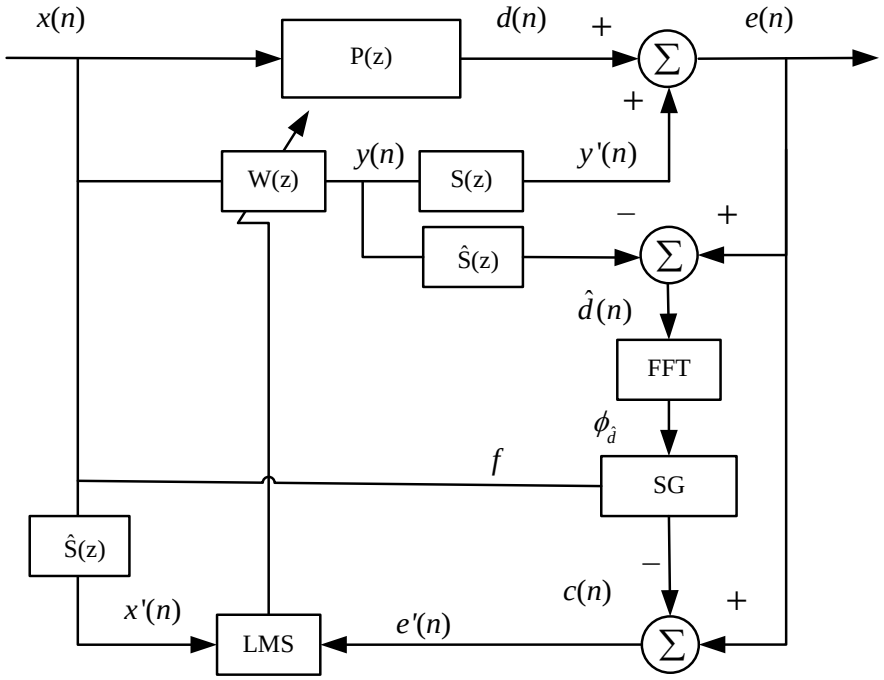


Figure 2. Block diagram of the PSC-FXLMS algorithm.

The characteristic of the PSC-FXLMS algorithm is setting the command signal in phase with the disturbance signal. The command signal phase is set by the measured phase by performing a fast Fourier transform (FFT) on the modeled disturbance. The modeled disturbance signal, $\hat{d}(n)$, can be expressed by

$$\hat{d}(n) = e(n) - y(n) * \hat{s}(n) \tag{7}$$

the FFT is performed to compute the phase of the disturbance signal, which is denoted as $\phi_{\hat{d}}$; then, the command signal can be expressed by:

$$c(n) = C\cos(2\pi f \frac{n}{Fs} + \phi_{\hat{d}}) \tag{8}$$

where C is the predefined amplitude of the command signal, Fs is the sampling rate and f is the frequency of the disturbance signal, which can be obtained from the reference signal.

2.3. Characteristic Equation With Phase Error

According to Equations (1)–(3) and (6), the mean square error (MSE) of the pseudo-error, which is related to the phase error, can be expressed by

$$\begin{aligned} \xi(n,\phi) &= E\left\{[e'(n)]^2\right\} \\ &= E\left\{[c(n) - d(n)]^2\right\} - 2\mathbf{p}(n,\phi)^T\mathbf{w}(n,\phi) + \mathbf{w}^T(n,\phi)\mathbf{R}(n)\mathbf{w}(n,\phi) \end{aligned} \tag{9}$$

where $E\{\cdot\}$ denotes the expected value, the $\mathbf{p}(n,\phi)$ is the desired-to-input cross-correlation vector at iterations n, when the phase error of the command signal and disturbance signal is ϕ and the $\mathbf{R}(n)$ is the input autocorrelation matrix, which are defined as follows

$$\mathbf{p}(n,\phi) = E\{[c(n) - d(n)]\mathbf{x}'(n)\} \tag{10}$$

$$\mathbf{R}(n) = E[\mathbf{x}'(n)\mathbf{x}'^{T}(n)] \tag{11}$$

According to the concept of steepest descent, the iteration with the phase error ϕ can be implemented into

$$\mathbf{w}(n+1,\phi) = \mathbf{w}(n,\phi) - \frac{\mu}{2}\nabla\xi(n,\phi) \tag{12}$$

where μ is the step size and vector $\nabla\xi(n,\phi)$ denotes the gradient of the error noise function. From Equation (9), the gradient can be easily calculated as follows

$$\nabla\xi(n,\phi) = -2\mathbf{p}(n,\phi) + 2\mathbf{R}(n)\mathbf{w}(n,\phi) \tag{13}$$

when the gradient is zero [i.e., $\nabla\xi(n,\phi) = 0$], the filter $\mathbf{w}(n,\phi)$ minimizes the MSE cost function $\xi(n,\phi)$ and the optimum of $\mathbf{w}(n,\phi)$ can be expressed as

$$\mathbf{w}^{o}(n,\phi) = \mathbf{p}(n,\phi)/\mathbf{R}(n) \tag{14}$$

where the $\mathbf{w}^{o}(n,\phi)$ is the expected optimum weight vector. Substituting Equation (14) into Equation (9), the minimum MSE $\xi_{\min}$ can be obtained

$$\xi_{\min} = E\left\{[c(n) - d(n)]^2\right\} - \mathbf{p}(n,\phi)^{T}\mathbf{w}^{o}(n,\phi) \tag{15}$$

then the MSE the pseudo-error can be calculated by

$$\xi(n,\phi) = \xi_{\min} + \widehat{\mathbf{w}}(n,\phi)^{T}\mathbf{R}(n)\widehat{\mathbf{w}}(n,\phi) \tag{16}$$

where the $\widehat{\mathbf{w}}(n,\phi)$ is the difference of the $\mathbf{w}(n,\phi)$ and $\mathbf{w}^{o}(n,\phi)$, and it is defined as

$$\widehat{\mathbf{w}}(n,\phi) = \mathbf{w}(n,\phi) - \mathbf{w}^{o}(n,\phi) \tag{17}$$

Substituting Equation (13) into Equation (12); the iteration is expressed as

$$\mathbf{w}(n+1,\phi) = [\mathbf{I} - \mu\mathbf{R}(n)]\mathbf{w}(n,\phi) + \mu\mathbf{p}(n,\phi) \tag{18}$$

Subtracting the optimum weight vector from both sides of the Equation (18) and according to the Equation (17), the process of the adaptive weight vector iteration can be equivalent to the iteration of the $\widehat{\mathbf{w}}(n,\phi)$, and it can be rewritten from Equation (18) and expressed as

$$\widehat{\mathbf{w}}(n+1,\phi) = [\mathbf{I} - \mu\mathbf{R}(n)]\widehat{\mathbf{w}}(n,\phi) \tag{19}$$

The autocorrelation matrix defined in Equation (11) can be decomposed into

$$\mathbf{R}(n) = \mathbf{Q}(n)\mathbf{\Lambda}(n)\mathbf{Q}^{T}(n) \tag{20}$$

where $\mathbf{\Lambda}(n) = diag[\lambda_0(n), \lambda_1(n), \ldots, \lambda_{L-1}(n)]$, $\mathbf{Q}(n)$ is the modal matrix formed by the eigenvectors of $\mathbf{R}(n)$ and it satisfies the following relationship: $\mathbf{I} = \mathbf{Q}(n)\mathbf{Q}^{T}(n)$.

A rotated weight misalignment vector can be defined by

$$\widetilde{\mathbf{w}}(n,\phi) = \mathbf{Q}^{T}(n)\widehat{\mathbf{w}}(n,\phi) \tag{21}$$

from Equation (19), it holds that:

$$\widetilde{\mathbf{w}}(n+1,\phi) = [\mathbf{I} - \mu\mathbf{\Lambda}(n)]\widetilde{\mathbf{w}}(n,\phi) \tag{22}$$

and

$$\widetilde{\mathbf{w}}(n,\phi) = [\mathbf{I} - \mu\mathbf{\Lambda}(n)]^{n}\widetilde{\mathbf{w}}(0,\phi) \tag{23}$$

Further, Equation (16) can be rewritten as follows

$$\xi(n,\phi) = \xi_{\min} + \widetilde{\mathbf{w}}(n,\phi)^T \mathbf{\Lambda}(n) \widetilde{\mathbf{w}}(n,\phi) \tag{24}$$

and

$$\begin{aligned} \xi(n,\phi) &= \xi_{\min} + \widetilde{\mathbf{w}}(0,\phi)^T [\mathbf{I} - \mu\mathbf{\Lambda}(n)]^n \mathbf{\Lambda}(n) [\mathbf{I} - \mu\mathbf{\Lambda}(n)]^n \widetilde{\mathbf{w}}(0,\phi) \\ &= \xi_{\min} + \sum_{l=0}^{L-1} \lambda_l(n) [1 - \mu\lambda_l(n)]^{2n} \widetilde{\mathbf{w}}_l^2(0,\phi) \end{aligned} \tag{25}$$

3. Performance Analysis

Theoretically, the amplitude of the command signal is the desired predefined value, while the phase of the command signal is unconcerned. However, in practice, for profiling the disturbance signal, while meeting the requirement for limiting the control effort simultaneously, the predefined command signal should be set to be in phase with the disturbance signal. Therefore, the PSC-FXLMS algorithm uses the FFT to estimate the phase of the modeled disturbance signal as an essential parameter for the command signal. In practical applications, an imperfectly modeled disturbance signal may lead to phase error between the command signal and the real disturbance signal. Therefore, the influence of the phase error between the command and disturbance signals on the convergence is explained in detail in the following section.

3.1. Control Effort

According to Equations (1) and (6), when the pseudo-error $e'(n)$ converges to zero, it holds that

$$y'(n) = c(n) - d(n) \tag{26}$$

where $y'(n)$ is the counter noise signal corresponding to the control effort. In the narrowband ANC systems, the command and disturbance signals can be considered as cosine waves. The phase error can be set as the difference in phase between the disturbance and command signals. Without loss of generality, the phase of the disturbance signal can be set to zero, and the phase of the command signal can be set as $\phi \in [0, 2\pi)$. The phase error between the command and disturbance signals is ϕ. The disturbance signal and the command signal can be written as

$$d(n) = D\cos(\omega n) \tag{27}$$

$$c(n) = C\cos(\omega n + \phi) \tag{28}$$

where ω is the circular frequency, and D and C are the amplitude of the disturbance signal and command signal, respectively. Substituting Equations (27) and (28) into Equation (26) yields

$$\begin{aligned} y'(n) &= C\cos(\omega n + \phi) - D\cos(\omega n) \\ &= C[\cos(\omega n)\cos\phi - \sin(\omega n)\sin\phi] - D\cos(\omega n) \\ &= [C\cos\phi - D]\cos(\omega n) - C\sin(\omega n)\sin\phi \\ &= Y'(C,\phi)\cos(\omega n + \phi') \end{aligned} \tag{29}$$

where $Y'(C,\phi)$ and ϕ' are amplitude and phase of the output $y'(n)$, respectively, and they are expressed as follows

$$Y'(C,\phi) = \sqrt{C^2 + D^2 - 2CD\cos\phi} \tag{30}$$

$$\phi' = \arctan\left(\frac{C\sin\phi}{C\cos\phi - D}\right) \tag{31}$$

The control effort is positively related to the amplitude of the output signal. Therefore, according to Equation (30), the control effort of the output is extremely relevant to the phase error ϕ. When $\phi : 0 \to \pi$, the control effort increases, and when $\phi : \pi \to 2\pi$, the control effort decreases. Thus, it is obvious that the control effort reaches a peak when $\phi = \pi$. These conclusions are identical to those presented in reference [13], and this paper presents an idea to estimate the control effort with the influence of phase error.

3.2. Convergence Time Constant

From Equation (25), it can be seen that $1 - \mu\lambda_l(n) < \mathbf{1}$, meaning that when $n \to \infty$, then $(1 - \mu\lambda_l(n))^{2n} \to 0$; from Equation (23), it can be easily obtained that when $n \to \infty$, then $\widetilde{\mathbf{w}}(n, \phi) \to \mathbf{0}$; that is, $\mathbf{w}(n, \phi) \to \mathbf{w}^o(n, \phi)$. Based on the basic knowledge about the sequence limit, it holds that $\widetilde{\mathbf{w}}(n, \phi) \to \mathbf{0}$ is equivalent to $\|\widetilde{\mathbf{w}}(n, \phi)\|_2 \to 0$. The norm $\| \ \|_2$ of Equation (23) is given by

$$\begin{aligned} \|\widetilde{\mathbf{w}}(n, \phi)\|_2 &= \left\|[\mathbf{I} - \mu\mathbf{\Lambda}(n)]^n \widetilde{\mathbf{w}}(0, \phi)\right\|_2 \\ &\leq \left\|[\mathbf{I} - \mu\mathbf{\Lambda}(n)]^n\right\|_2 \|\widetilde{\mathbf{w}}(0, \phi)\|_2 \\ &= [1 - \mu\lambda_{\min}(n)]^n \|\widetilde{\mathbf{w}}(0, \phi)\|_2 \\ &\leq [1 - \mu\lambda_{\min}(n)]^n \left\|\mathbf{Q}^T(n)\right\|_2 [\|\mathbf{w}^o(n, \phi)\|_2 + \|\mathbf{w}(0, \phi)\|_2] \end{aligned} \tag{32}$$

Further, based on the knowledge about the LIMIT, the problem $\|\widetilde{\mathbf{w}}(n, \phi)\|_2 \to 0$ can be defined as follows. For any $\varepsilon > 0$, there exists an N such that when $n > N$, it holds that $\|\widetilde{\mathbf{w}}(n, \phi)\|_2 < \varepsilon$. In practice, a real constant $\varepsilon_0 \ll 1$ can be defined, and when $n > N$, then $\|\widetilde{\mathbf{w}}(n, \phi)\|_2 < \varepsilon_0$, which means that $\|\widetilde{\mathbf{w}}(n, \phi)\|_2$ has converged. That is, when

$$[1 - \mu\lambda_{\min}(n)]^n \left\|\mathbf{Q}^T(n)\right\|_2 [\|\mathbf{w}^o(n, \phi)\|_2 + \|\mathbf{w}(0, \phi)\|_2] < \varepsilon_0 \tag{33}$$

the norm $\|\widetilde{\mathbf{w}}(n, \phi)\|_2$ has converged. From the Equations (2) and (4), The required Z-transform of $e'(n)$ is denoted as $E'(z)$ and is expressed as

$$E'(z) = D(z) + Y(z)S(z) - C(z) \tag{34}$$

where $D(z)$, $Y(z)$ and $C(z)$ are the Z-transformations of the disturbance signal, output signal and command signal, respectively. Substituting the Z-transformations of Equation (3) into Equation (6), the $E'(z)$ can be expressed as

$$E'(z) = D(z) + W(z)X(z)S(z) - C(z) \tag{35}$$

It can be seen that when the pseudo-error signal converges to zero, [i.e., $E'(z) = 0$], which indicates that $W(z)$ realized the optimal transfer function

$$W^o(z) = \frac{C(z) - D(z)}{X(z)S(z)} = \frac{C(z) - D(z)}{X'(z)} \tag{36}$$

where the superscript "o" indicates the optimum value. Then the magnitude of the optimal weight vector is expressed as

$$\|\mathbf{w}^o(n, \phi)\|_2 = \frac{\sqrt{C^2 + D^2 - 2CD\cos\phi}}{|X'|} \tag{37}$$

where $|X'|$ is the magnitude of the filtered reference signal. From Equations (32) and (37), and because the positive value of $\|\mathbf{w}^o(n, \phi)\|_2$, the magnitude of $\|\widetilde{\mathbf{w}}(n, \phi)\|_2$ is expressed as

$$\|\widetilde{\mathbf{w}}(n, \phi)\|_2 = [1 - \mu\lambda_{\min}(n)]^n \left\|\mathbf{Q}^T(n)\right\|_2 \left[\frac{\sqrt{C^2 + D^2 - 2CD\cos\phi}}{|X'|} + \|\mathbf{w}(0, \phi)\|_2\right] \tag{38}$$

It can be seen that when the system is converged, the magnitude satisfies

$$[1 - \mu\lambda_{\min}(n)]^n M(n,\phi) < \varepsilon_0 \tag{39}$$

where the ε_0 is a very small constant, and the $M(n,\phi)$ is defined as

$$M(n,\phi) = \left\|\mathbf{Q}^T(n)\right\|_2 \left[\frac{\sqrt{C^2 + D^2 - 2CD\cos\phi}}{|X'|} + \|\mathbf{w}(0,\phi)\|_2\right] \tag{40}$$

Therefore, the number of iterations which satisfied convergence is given by

$$n_0(\phi) = \log_{1-\mu\lambda_{\min}(n)}[\varepsilon_0 / M(n,\phi)] \tag{41}$$

Since the iterations is a positive integer, the number of iterations can be written as

$$N(\phi) = [n_0(\phi)] + 1 \tag{42}$$

where $[n_0(\phi)]$ indicates that $n_0(\phi)$ is rounded down.

From the above expressions, the following conclusions can be drawn:

(1) For stationary signals, according to Equations (38)–(42), when the sequence $\|\widetilde{\mathbf{w}}[N(\phi),\phi]\|_2 < \varepsilon_0$ is satisfied, then $\mathbf{w}(n,\phi) \approx \mathbf{w}^o(n,\phi), n = N(\phi)+1, N(\phi)+2, \cdots$. Additionally, $N(\phi)$ indicates the iteration number of the weight vector $\mathbf{w}(n,\phi)$ from $\mathbf{w}(0,\phi)$ to $\mathbf{w}^o(n,\phi)$, which corresponds to the convergence of the MSE from $\xi(0,\phi)$ to $\xi_{\min}$. The iteration number $N(\phi)$ is related to the phase error ϕ. Based on Equation (37), the relationship is as follows: when $\phi : 0 \to \pi$, $N(\phi)$ increases progressively, and when $\phi : \pi \to 2\pi$, $N(\phi)$ decreases progressively. Thus, the iteration number $N(\phi)$ reaches a peak when $\phi = \pi$. Consequently, in real applications, there can be a large convergence time constant when the disturbance and command signals are out of phase.

(2) According to Equations (14) and (37), the phase error ϕ has an impact of $\|\mathbf{w}^o(n,\phi)\|_2 > \|\mathbf{w}^o(n,0)\|_2$. Combining this with Equation (38), it can be concluded that the phase error increases the norm of vector $\|\widetilde{\mathbf{w}}(n,\phi)\|_2$; in other words, the phase error ϕ may increase the convergence time constant by resulting in a $\mathbf{w}^o(n,\phi)$ more distant from $\mathbf{w}(0,\phi)$. From Equations (37)–(42), it can be seen that, if the value of $\|\widetilde{\mathbf{w}}(n,\phi)\|_2$ is large, the iteration number $N(\phi)$ is also large, which implies a large convergence time constant.

3.3. Convergence Performance Analysis

As mentioned above, in the process of $\|\widetilde{\mathbf{w}}(n,\phi)\|_2 \to 0$, the iteration focuses on the MSE difference given by Equation (25). The difference of $\xi(n,\phi)$ can be defined as follows:

$$\begin{aligned}\Delta\xi(n,\phi) &= \xi(n+1,\phi) - \xi(n,\phi)\\ &= \sum_{l=0}^{L-1}\lambda_l(n)[1-\mu\lambda_l(n)]^{2n+2}\widetilde{w}_l^2(0,\phi) - \sum_{l=0}^{L-1}\lambda_l(n)[1-\mu\lambda_l(n)]^{2n}\widetilde{w}_l^2(0,\phi)\\ &= -2\mu\sum_{l=0}^{L-1}\lambda_l^2(n)[1-\mu\lambda_l(n)]^{2n}\widetilde{w}_l^2(0,\phi) + \mu^2\sum_{l=0}^{L-1}\lambda_l^3(n)[1-\mu\lambda_l(n)]^{2n}\widetilde{w}_l^2(0,\phi)\end{aligned} \tag{43}$$

when the iteration is far from the convergence, $\Delta\xi(n,\phi) < 0, \forall n$, and according to the Lyapunov stability theory, the smaller the difference of the Lyapunov function is, the faster the system convergence speed is. Therefore, according to $\|\mathbf{w}^o(n,\phi)\|_2 > \|\mathbf{w}^o(n,0)\|_2$, the phase error ϕ satisfies the condition of $\Delta\xi(n,\phi) < \Delta\xi(n,0)$, leading to a faster convergence speed when the command and disturbance signals are out of phase. However, due to the slow adaptation and the fact that $\mu \ll 1$, $\Delta\xi(n,\phi)$ is mostly determined by μ and slightly by $\widetilde{w}_l^2(0,\phi)$. Therefore, the increase in the convergence rate due to the phase error is minimal, and even negligible. Consequently, the command signal and disturbance signal being out of phase may lead to an inevitable increase in the convergence time constant.

From Equation (25), it can be seen that the MSE is influenced by the phase error ϕ, and a ratio can be defined by

$$\eta = \frac{\xi(n,\phi)}{\xi(n,0)} = \frac{\xi_{\min} + \sum_{l=0}^{L-1} \lambda_l(n)[1-\mu\lambda_l(n)]^{2n}\widetilde{w}_l^2(0,\phi)}{\xi_{\min} + \sum_{l=0}^{L-1} \lambda_l(n)[1-\mu\lambda_l(n)]^{2n}\widetilde{w}_l^2(0,0)} \tag{44}$$

Without loss of generality, the initial value of weight vector can be set as $\mathbf{w}(0,\phi) = 0$; then, from Equation (37), it can be imprecisely obtained:

$$\frac{\mathrm{w}_l^o(n,\phi)}{\mathrm{w}_l^o(n,0)} = \sqrt{\frac{C^2 + D^2 - 2CD\cos\phi}{(C-D)^2}} = \alpha \tag{45}$$

where the α is defined as a ratio related to the phase error. The Equation (44) can be rewritten as

$$\eta = \frac{\xi(n,\phi)}{\xi(n,0)} = \frac{\xi_{\min} + \alpha^2 \sum_{l=0}^{L-1} \lambda_l(n)[1-\mu\lambda_l(n)]^{2n}}{\xi_{\min} + \sum_{l=0}^{L-1} \lambda_l(n)[1-\mu\lambda_l(n)]^{2n}} \tag{46}$$

When the algorithm is far from the steady state, assuming that $\xi_{\min}$ is negligibly small, the ratio given by Equation (46) can be expressed as follows:

$$\eta = \frac{\xi_{\min} + \alpha^2 \sum_{l=0}^{L-1} \lambda_l(n)[1-\mu\lambda_l(n)]^{2n}}{\xi_{\min} + \sum_{l=0}^{L-1} \lambda_l(n)[1-\mu\lambda_l(n)]^{2n}} \approx \frac{\alpha^2 \sum_{l=0}^{L-1} \lambda_l(n)[1-\mu\lambda_l(n)]^{2n}}{\sum_{l=0}^{L-1} \lambda_l(n)[1-\mu\lambda_l(n)]^{2n}} = \alpha^2 \tag{47}$$

Therefore, the phase error has nonnegligible influence on convergence performance when adaption is far from the steady state. This coincides with the conclusion that the phase error may increase the convergence time constant by resulting in a $\mathbf{w}^o(n,\phi)$ that is distant from $\mathbf{w}(0,\phi)$. The term $[1-\mu\lambda_l(n)]^{2n}$ converges to zero, as the adaptive filter converges. As given in Equation (44), the $\xi(n,\phi)$ converges to $\xi_{\min}$, and the ratio η converges to one. Consequently, the MSE performance at the steady state is slightly affected by the phase error ϕ.

For nonstationary signals, according to Equation (14), the optimum weight vector $\mathbf{w}_{non}^o(n,\phi)$ is time-varying. In other words, the adaptive vector $\mathbf{w}_{non}(n,\phi)$ converges to a time-varying objective with every updating step. Then, the iteration of Equation (18) can be regarded as a one-step steepest descent update. In cases far from convergence, and when the changing speed of $\mathbf{w}_{non}^o(n,\phi)$ is much slower than the adaption speed of $\mathbf{w}_{non}(n,\phi)$, it can be assumed that $\mathbf{w}_{non}^o(n+1,\phi) \approx \mathbf{w}_{non}^o(n,\phi)$, and the MSE also, can be expressed by Equation (25). Under these assumptions, the following approximation can be made based on Equations (16)–(19), (23)–(24):

$$\begin{aligned} \xi(n+1,\phi) &\approx \xi_{\min} + \widetilde{\mathbf{w}}_{non}(n,\phi)^T[\mathbf{I}-\mu\mathbf{\Lambda}(n)]\mathbf{\Lambda}(n)[\mathbf{I}-\mu\mathbf{\Lambda}(n)]\widetilde{\mathbf{w}}_{non}(n,\phi) \\ &\approx \xi_{\min} + \sum_{l=0}^{L-1} \lambda_l(n)[1-\mu\lambda_l(n)]^2 \widetilde{w}_{non,l}^2(n,\phi) \end{aligned} \tag{48}$$

The Equation (48) is similar to Equation (25), and the difference of $\xi(n,\phi)$ in the nonstationary case can be expressed by

$$\Delta\xi(n,\phi) = -2\mu \sum_{l=0}^{L-1} \lambda_l(n)\widetilde{w}_{non,l}^2(n,\phi) + \mu^2 \sum_{l=0}^{L-1} \lambda_l^2(n)\widetilde{w}_{non,l}^2(n,\phi) \tag{49}$$

which implies that the convergence rate of a one-step adaption may have some influence from the phase error. In one-step adaption, the phase error leads to a slight increase in convergence rate. However, as the adaptive vector updates, the optimum of $\mathbf{w}_{non}^{o}(n,\phi)$ is time-varying, and there may be an influence of the adaptive filter reaching the optimum at every step. This may make the estimation of the influence difficult, or even impossible. However, as with the stationary case, due to the domination of μ for the convergence rate, the influence on the convergence rate due to the phase error is minimal, and even negligible. Consequently, the phase error ϕ may result in an inevitable increase in the convergence time constant.

To investigate the effect of the phase error on a nonstationary system more clearly, a ratio β can be defined by

$$\beta = \frac{\xi(n,\phi)}{\xi(n,0)} = \frac{\xi_{\min} + \sum_{l=0}^{L-1} \lambda_l(n)[1-\mu\lambda_l(n)]^{2n}\widetilde{w}_{non,l}^{2}(n,\phi)}{\xi_{\min} + \sum_{l=0}^{L-1} \lambda_l(n)[1-\mu\lambda_l(n)]^{2n}\widetilde{w}_{non,l}^{2}(n,\phi)} \tag{50}$$

Assuming that the change in the optimum of $\mathbf{w}_{non}^{o}(n,\phi)$ is linear or quasi-linear, the ratio β can be rewritten similarly to Equation (46):

$$\beta = \frac{\xi_{\min} + \sum_{l=0}^{L-1} \lambda_l(n)[1-\mu\lambda_l(n)]^{2n}\widetilde{w}_{non,l}^{2}(n,\phi)}{\xi_{\min} + \sum_{l=0}^{L-1} \lambda_l(n)[1-\mu\lambda_l(n)]^{2n}\widetilde{w}_{non,l}^{2}(n,\phi)} \approx \frac{\xi_{\min} + \alpha^2 \sum_{l=0}^{L-1} \lambda_l(n)[1-\mu\lambda_l(n)]^{2n}}{\xi_{\min} + \sum_{l=0}^{L-1} \lambda_l(n)[1-\mu\lambda_l(n)]^{2n}} \tag{51}$$

Similarly, at the far-from-steady state, the $\xi_{\min}$ is always negligibly small, and the ratio given by Equation (51) can be expressed as follows:

$$\beta = \frac{\xi_{\min} + \alpha^2 \sum_{l=0}^{L-1} \lambda_l(n)[1-\mu\lambda_l(n)]^{2n}}{\xi_{\min} + \sum_{l=0}^{L-1} \lambda_l(n)[1-\mu\lambda_l(n)]^{2n}} \approx \alpha^2 \tag{52}$$

therefore, the phase error has nonnegligible influence on convergence performance at the far-from-steady state. This conclusion is identical to that of stationary cases. As the adaptive filter converges, the term $[1-\mu\lambda_l(n)]^{2n}$ converges to zero, and the ratio β converges to one. Consequently, the MSE performance at the steady state is slightly affected by the phase error ϕ.

4. Simulations

In this section, the simulation results for three cases are provided to clarify the insights into the influence of the phase error. In cases 1 and 2, simulations were conducted to demonstrate the validity of the derived convergence time constant performance and steady state MSE expressions. The primary and secondary paths were FIR filters created with the MATLAB function (fir1) with cutoff frequencies of 0.4π and 0.5π, respectively. The disturbance signal and command signal were defined by Equations (27) and (28), and the amplitudes of the disturbance and command signals were D = 2 and C =1, respectively. In case 3, the influence of phase error was demonstrated with an application of the algorithm of nonstationary noise profiling in reference [15]. The primary path P(z) and secondary path S(z) were extracted from a real acoustic duct system, which was shown in Figure 4 in [15], and their impulse response and frequency response were shown in Figure 4 in [15]. The simulation noise was the same as the case C1 in [15], in which the chirp rate is 10.

4.1. Case 1

This case considered the stationary disturbance. The step size of the FXLMS was 0.000005. The frequency of the disturbance signal was set to 120 Hz, and the phase error was in turn set to $\phi = 0,\ \pi/4,\ \pi/2,\ \pi$. The MSE of the pseudo-error under different phase errors is presented in Figure 3. It can be seen that the convergence time constant increased when the phase error changed from zero to π. However, the MSE performances of the pseudo-error at the steady state were nearly identical to each other. In addition, the estimation results when the command and disturbance signals were out of phase are shown simultaneously. It can be seen that the ratio of Equation (46) provided an excellent estimation of the performance when the command signal was out of phase with the disturbance signal, both at the convergence stage and the steady state.

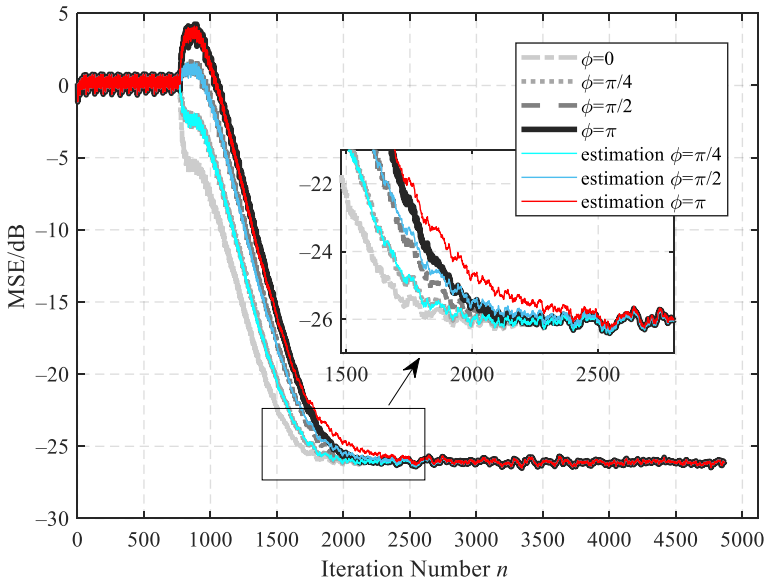


Figure 3. The MSE result of the pseudo-error for different iteration numbers under different phase errors.

As shown in Figure 4, at the convergence stage, the difference $\Delta\xi(n,\phi)$ under different phase errors decreased when the phase error increased from zero to π, which implied that the phase error increased the convergence rate, as given in Equation (43). However, as shown in Figures 3 and 4, the MSE difference under different phase errors $[\xi(n,\phi) - \xi(n,0)]$ was large, and this increase in the convergence rate was insufficient to counteract the considerable disparity, due to which the phase error led to $\mathbf{w}^o(n,\phi)$ being far from $\mathbf{w}(0,\phi)$. The adaptation of $\|\mathbf{w}^o(n,\phi)\|_2$ under different phase errors $[\mathbf{w}(0,\phi) = 0]$ is presented in Figure 5, where the norm $\|\mathbf{w}^o(n,\phi)\|_2$ increased when the phase error changed from zero to π. The convergence time constant result of $\mathbf{w}(n,\phi)$, which represented a change from $\mathbf{w}(0,\phi)$ to $\mathbf{w}^o(n,\phi)$, was in accordance with the performance presented by the MSE of the pseudo-error.

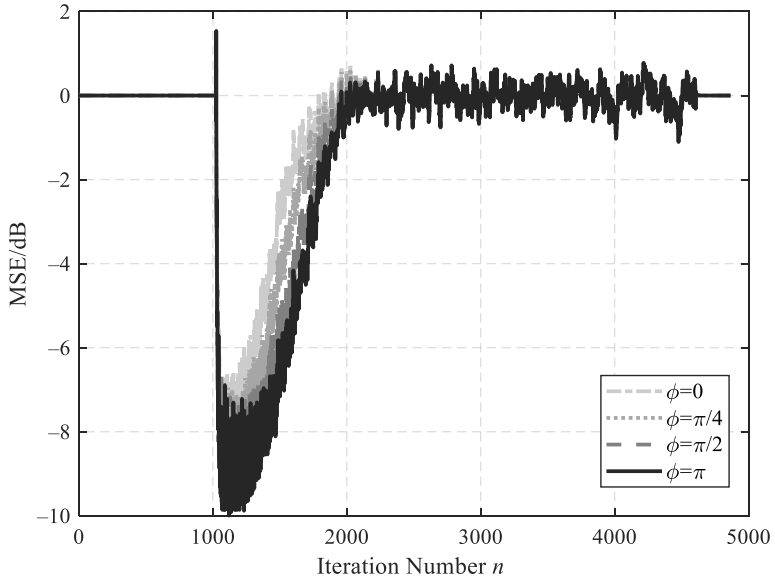


Figure 4. Difference of $\xi(n, \phi)$ under different phase errors.

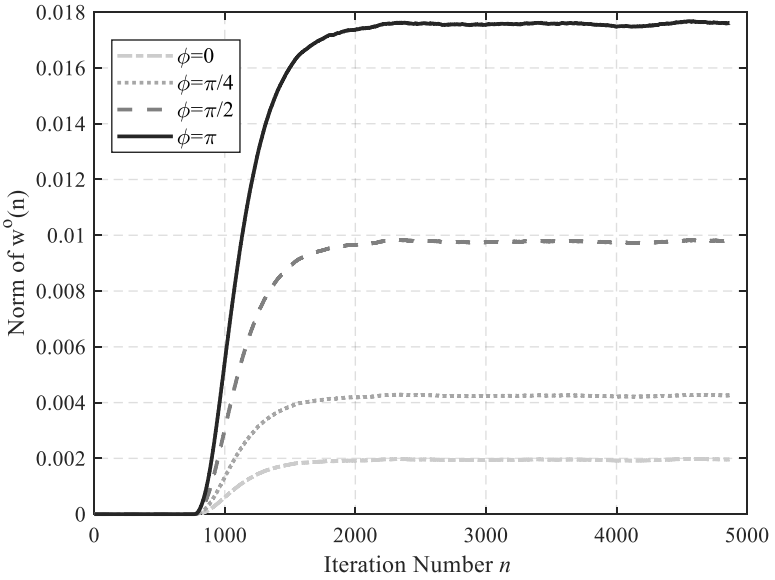


Figure 5. The adaptation of $\|\mathbf{w}^o(n, \phi)\|_2$ under different phase errors ($\mathbf{w}(0, \phi) = \mathbf{0}$).

4.2. Case 2

This case considered the nonstationary disturbance. The frequency of the disturbance signal changed linearly from 30 Hz to 150 Hz and from 150 to 30 Hz, and the phase error was, in turn, set to $\phi = 0,\ \pi/4,\ \pi/2,\ \pi$. The step size of the FXLMS was 0.000005, and the background noise was set to zero. The performances of the pseudo error MSE under different phase errors when the frequency of disturbance signal changed from 30 Hz to 150 Hz and from 150 Hz to 30 Hz are presented in Figures 6 and 7, respectively. It can be seen that the phase error significantly decreased the performance of the adaptive system. Because the step size was very small, the adaption was approximate in the convergence stage (far-from-steady state), causing the pseudo-error MSE of $\phi = \pi$ to always be short of even 10 dB compared to the pseudo-error MSE of $\phi = 0$. Additionally, according to Equation (52), the estimation results when the command and disturbance signals were out of phase are shown in Figures 6 and 7, respectively. It can be seen that the ratio of Equation (52) provided a satisfactory estimation of the performance when the command signal was out of phase with the disturbance signal. However, there was a certain discrepancy

between the predicted and simulated performance, and the discrepancy seemed to continue to grow as the iteration progressed. This phenomenon may be generated by the imprecise assumption of Equation (45) and the subjective judgement of when the adaption is far from the steady state.

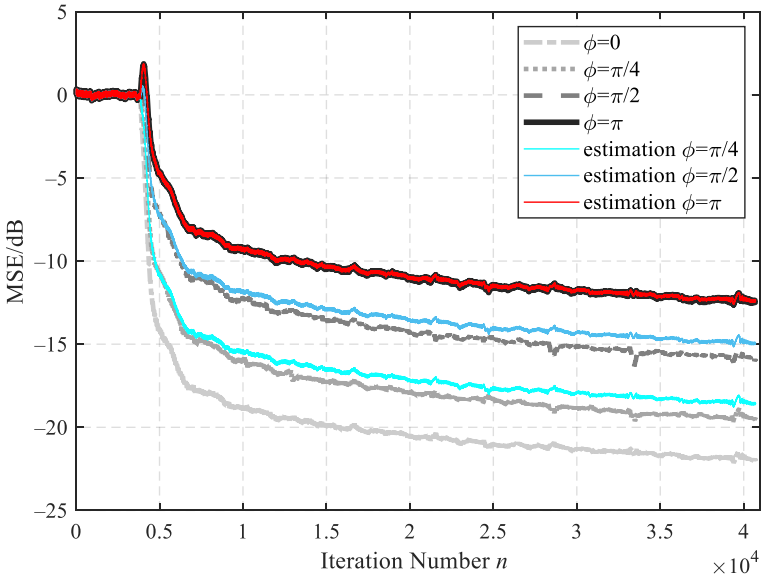


Figure 6. The MSE of the pseudo-error under different phase errors when f changes from 30 Hz to 150 Hz.

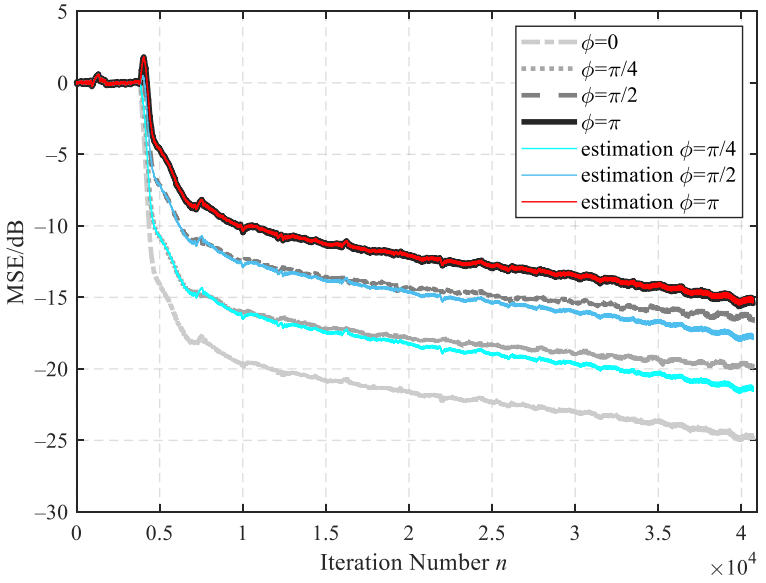


Figure 7. The MSE of the pseudo-error under different phase errors when f changes from 150 Hz to 30 Hz.

In addition, to demonstrate the convergence process of the adaption and decrease the convergence time constant to a steady state, the step size was set to a linear change from 0.000005 to 0.000022 as the adaption proceeded. The background noise was set as white noise with a mean square error of 0.2. The performances of the pseudo-error MSE under different phase errors when the frequency of disturbance signal changed from 30 Hz to 150 Hz and from 150 Hz to 30 Hz are presented in Figures 8 and 9, respectively. It can be seen that the phase error significantly increased the convergence time constant to the steady state. Simultaneously, the estimation results according to Equation (51) were satisfactory at

both the far-from-steady state and the steady state of adaption. The deviation from about iteration 7500 to 22,500 may be generated by the imprecise assumption of Equation (45) and the linear change in optimum of $\mathbf{w}_{non}^{o}(n, \phi)$.

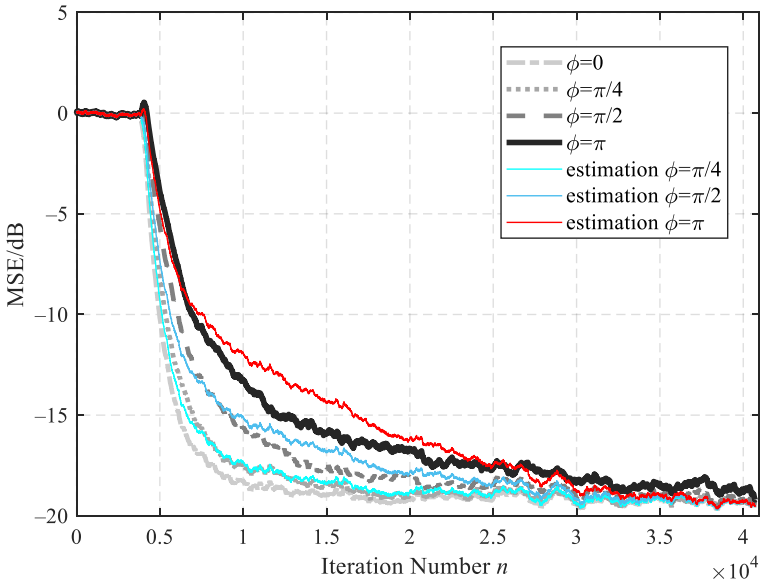


Figure 8. The MSE of the pseudo-error under different phase errors when f changes from 30 Hz to 150 Hz. The step size was set to a linear change from 0.000005 to 0.000022.

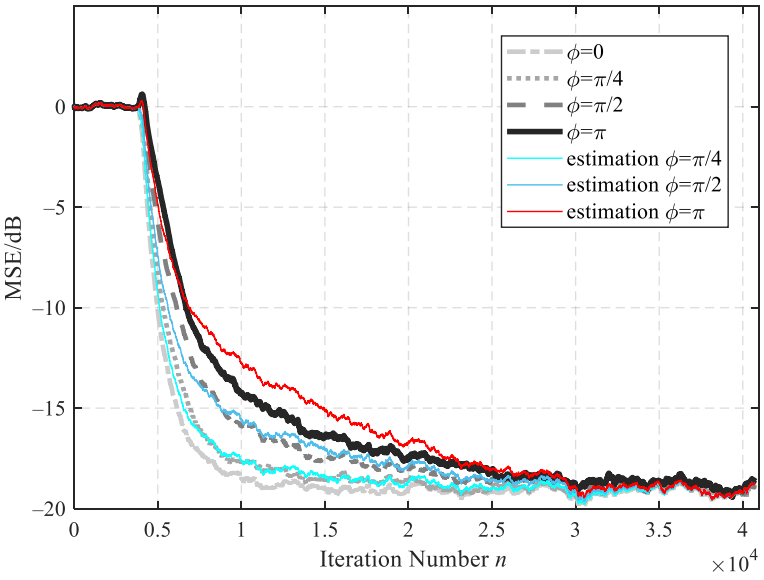


Figure 9. The MSE of the pseudo-error under different phase errors when f changes from 150 Hz to 30 Hz. The step size was set to a linear change from 0.000005 to 0.000022.

4.3. Case 3

In this case, a real acoustic duct system was used, and the active sound profiling algorithm was employed to obtain the influence of the phase error, as mentioned above. The ASP performance under different phase errors in the steady state is shown in Figure 10. When the command signal was in phase with the disturbance signal, as shown in Figure 10a, there was a superior control performance, reducing the disturbance amplitude range from approximately 24 dB to less than 4 dB. When the phase error increased, as shown in Figure 10b–d, the profiled sound (error signal) limit had a significant decrease in perfor-

mance. The results indicated that the out of phase between command and disturbance signals could be adverse to the main objective of profiling the nonstationary noise.

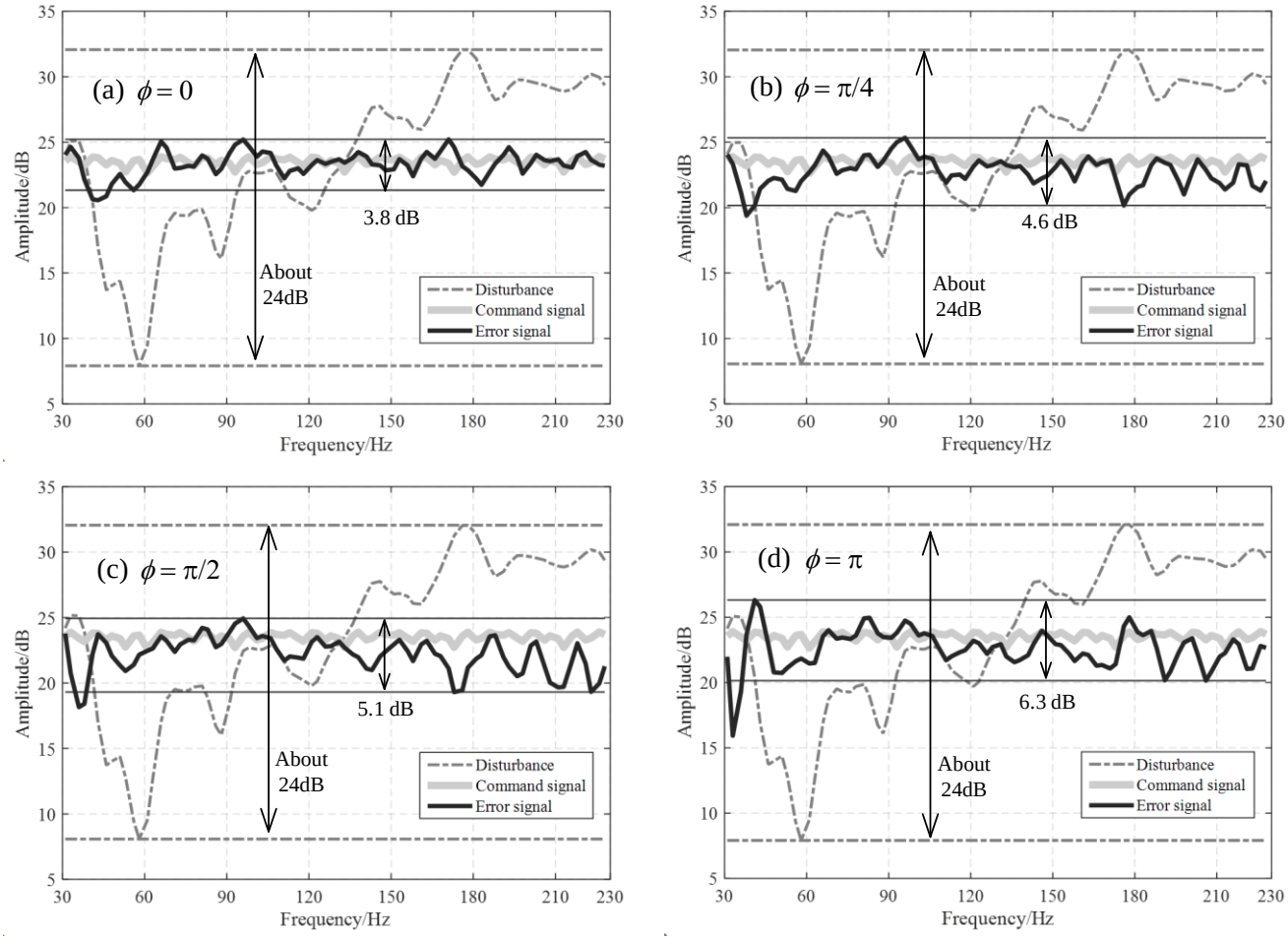


Figure 10. The ASP performance under different phase errors: (**a**) $\phi = 0$, (**b**) $\phi = \pi/4$, (**c**) $\phi = \pi/2$ and (**d**) $\phi = \pi$.

5. Conclusions

In this study, a detailed analysis of the PSC-FXLMS algorithm with phase error between the disturbance and command signals was conducted. The influence of the phase error on control effort, the convergence time constant and convergence behavior have been discussed in both stationary and nonstationary disturbance cases. It can be concluded, for both stationary and nonstationary disturbance, that the phase error may heavily increase the distance of the optimum vector from the initial value, leading to a large control effort, a large convergence time constant and poor convergence performance. An estimation ratio, in both stationary and nonstationary disturbance cases, of the pseudo-error MSE convergence performance has also been developed and discussed. The analytical findings and results are supported by extensive simulations.

Author Contributions: Conceptualization, Y.W. and F.L.; methodology, Y.W.; validation, F.L., Z.F. and L.Y.; formal analysis, L.Y.; investigation, Y.W.; resources, Y.W.; data curation, Y.W.; writing—original draft preparation, Y.W.; writing—review and editing, P.W.; visualization, Y.W.; supervision, Y.W.; project administration, Y.W.; funding acquisition, Y.W. All authors have read and agreed to the published version of the manuscript.

Funding: This research received no external funding.

Institutional Review Board Statement: Not applicable.

Informed Consent Statement: Not applicable.

Data Availability Statement: Some or all data, models, or codes generated or used during the study are proprietary or confidential in nature and may only be provided with restrictions.

Conflicts of Interest: The authors declare no conflict of interest.

References

1. De Oliveira, L.P.R. Review and future perspectives on active sound quality control. In Proceedings of the ISMA 2010—International Conference on Noise and Vibration Engineering Including USD 2010, Leuven, Belgium, 20–22 September 2010; pp. 177–191.
2. Sano, H.; Inoue, T.; Takahashi, A.; Terai, K.; Nakamura, Y. Active control system for low-frequency road noise combined with an audio system. *IEEE Trans. Speech Audio Process.* **2001**, *9*, 755–763. [CrossRef]
3. Pinte, G.; Stallaert, B.; Sas, P.; Desmet, W.; Swevers, J. A novel design strategy for iterative learning and repetitive controllers of systems with a high modal density: Theoretical background. *Mech. Syst. Sig. Process.* **2010**, *24*, 432–443. [CrossRef]
4. Stallaert, B.; Pinte, G.; Sas, P.; Desmet, W.; Swevers, J. A novel design strategy for iterative learning and repetitive controllers of systems with a high modal density: Application to active noise control. *Mech. Syst. Signal Proc.* **2010**, *24*, 444–454. [CrossRef]
5. Gonzalez, A.; Ferrer, M.; de Diego, M.; Pinero, G.; Garcia-Bonito, J.J. Sound quality of low-frequency and car engine noises after active noise control. *J. Sound Vib.* **2003**, *265*, 663–679. [CrossRef]
6. Ardekani, I.T.; Abdulla, W.H. Theoretical convergence analysis of FxLMS algorithm. *Signal Process.* **2010**, *90*, 3046–3055. [CrossRef]
7. Ma, Y.; Xiao, Y.; Ma, L.; Khorasani, K. Statistical analysis of narrowband active noise control using a simplified variable step-size FXLMS algorithm. *Signal Process.* **2021**, *183*, 108012. [CrossRef]
8. Ji, M.J.; Kuo, S.M. An active harmonic noise equalizer. In Proceedings of the 1993 IEEE International Conference on Acoustics, Speech, and Signal Processing, Minneapolis, MN, USA, 27–30 April 1993; Volume 181, pp. 189–192.
9. Kuo, S.M.; Ji, M.J. Development and analysis of an adaptive noise equalizer. *IEEE Trans. Speech Audi Process.* **1995**, *3*, 217–222. [CrossRef]
10. Liu, F.; Mills, J.K.; Dong, M.M.; Gu, L. Active broadband sound quality control algorithm with accurate predefined sound pressure level. *Appl. Acoust.* **2017**, *119*, 78–87. [CrossRef]
11. Feng, J.W.; Gan, W.S. Adaptive active noise equalizer. *Electron. Lett.* **1997**, *33*, 1518–1519. [CrossRef]
12. Feng, J.W.; Gan, W.S. A broadband self-tuning active noise equaliser. *Signal Process.* **1997**, *62*, 251–256. [CrossRef]
13. Rees, L.E.; Elliott, S.J. Adaptive algorithms for active sound-profiling. *IEEE Trans. Audio Speech Lang. Process.* **2006**, *14*, 711–719. [CrossRef]
14. Patel, V.; Cheer, J.; George, N.V. Modified phase-scheduled-command FxLMS algorithm for active sound profiling. *IEEE-ACM Trans. Audio Speech Lang. Process.* **2017**, *25*, 1495–1504. [CrossRef]
15. Wang, Y.; Gu, L.; Liu, F.; Dong, M. An adaptive algorithm for nonstationary active sound-profiling. *Appl. Acoust.* **2018**, *137*, 51–61. [CrossRef]
16. Wang, Y.; Gu, L.; Liu, F.; Dong, M. Online secondary path modeling for active sound quality control systems. *Appl. Acoust.* **2019**, *155*, 44–52. [CrossRef]
17. Kuo, S.M.; Mallu, S. Adaptive active sound quality control algorithm. In Proceedings of the 2005 International Symposium on Intelligent Signal Processing and Communication Systems, Hong Kong, China, 13–16 December 2005; pp. 737–740.
18. Kuo, S.M.; Gupta, A.; Mallu, S. Development of adaptive algorithm for active sound quality control. *J. Sound Vib.* **2007**, *299*, 12–21. [CrossRef]
19. Kuo, S.M.; Yenduri, R.K.; Gupta, A. Frequency-domain delayless active sound quality control algorithm. *J. Sound Vib.* **2008**, *318*, 715–724. [CrossRef]
20. De Oliveira, L.P.R.; Stallaert, B.; Janssens, K.; Van der Auweraer, H.; Sas, P.; Desmet, W. NEX-LMS: A novel adaptive control scheme for harmonic sound quality control. *Mech. Syst. Sig. Process.* **2010**, *24*, 1727–1738. [CrossRef]
21. Mosquera-Sanchez, J.A.; Desmet, W.; De Oliveira, L.P.R. Multichannel feedforward control schemes with coupling compensation for active sound profiling. *J. Sound Vib.* **2017**, *396*, 1–29. [CrossRef]
22. Mosquera-Sanchez, J.A.; Sarrazin, M.; Janssens, K.; de Oliveira, L.P.R.; Desmet, W. Multiple target sound quality balance for hybrid electric powertrain noise. *Mech. Syst. Sig. Process.* **2018**, *99*, 478–503. [CrossRef]
23. Mosquera-Sanchez, J.A.; Desmet, W.; De Oliveira, L.P.R. A multichannel amplitude and relative-phase controller for active sound quality control. *Mech. Syst. Sig. Process.* **2017**, *88*, 145–165. [CrossRef]
24. Liu, J.X.; Chen, X.F. Adaptive Compensation of Misequalization in Narrowband Active Noise Equalizer Systems. *IEEE/ACM Trans. Audio Speech Lang. Process.* **2016**, *24*, 2390–2399. [CrossRef]
25. Wang, L.; Gan, W.S. Analysis of misequalization in a narrowband active noise equalizer system. *J. Sound Vib.* **2008**, *311*, 1438–1446. [CrossRef]

Disclaimer/Publisher's Note: The statements, opinions and data contained in all publications are solely those of the individual author(s) and contributor(s) and not of MDPI and/or the editor(s). MDPI and/or the editor(s) disclaim responsibility for any injury to people or property resulting from any ideas, methods, instructions or products referred to in the content.